Transversely isotropic tensile material properties of skeletal muscle tissue

Duane A. Morrow, MS[1,2], **Tammy L. Haut Donahue, PhD**[2], **Gregory M. Odegard**[2], and **Kenton R. Kaufman, PhD, PE**[1,2]

[1] Motion Analysis Laboratory, Division of Orthopedic Research, Mayo Clinic, Rochester, MN, USA.

[2] Department of Mechanical Engineering – Engineering Mechanics, Michigan Technological University, Houghton, MI, USA

Keywords

Skeletal Muscle; Material Properties; Transverse Isotropy; Tensile Behavior

INTRODUCTION

Measurement of individual muscle performance could allow for the monitoring of disease progression, evaluation of therapeutic intervention efficacy, and improvement in the understanding of how various conditions affect muscle function. In the absence of direct measurement of individual muscle function, investigators have used computational models to try and fill gaps in knowledge. Models of skeletal muscle have advanced from unidirectional Hill-type muscle model introduced in 1938 (Hill, 1938) to three-dimensional continuum-based muscle models that have been developed more recently (Blemker and Delp, 2005, Gielen, et al., 2000, Jenkyn, et al., 2002, Johansson, et al., 2000, Martins, et al., 1998, Odegard, et al., 2008, Yucesoy, et al., 2002). Regardless of the level of complexity, the inherent validity of a model is tied to the material properties used to determine model parameters. Given this, it is surprising to note the relative lack of studies examining the material properties of skeletal muscle tissue.

From the arrangement of skeletal muscle architecture (i.e., the parallel bundling of serially-arranged muscle fibers), it has been hypothesized that skeletal muscle can be considered transversely isotropic (Blemker and Delp, 2005) with the fiber (longitudinal) axis defining the plane of symmetry. A transversely isotropic material may be fully characterized by testing the tissue under longitudinal extension (LE), transverse extension (TE), and longitudinal shear (LS). Of the investigators who have looked to characterize muscle in the fiber direction (Anderson, et al., 2002, Anderson, et al., 2001, Boriek, et al., 2001, Gosselin, et al., 1998, Hete

Corresponding Author: Dr. Kenton R. Kaufman, Motion Analysis Lab, 200 First Street SW, Rochester, MN 55905, USA, Phone: 507-284-2262, Fax: 507-266-2227, Email: kaufman.kenton@mayo.edu.

Publisher's Disclaimer: This is a PDF file of an unedited manuscript that has been accepted for publication. As a service to our customers we are providing this early version of the manuscript. The manuscript will undergo copyediting, typesetting, and review of the resulting proof before it is published in its final citable form. Please note that during the production process errors may be discovered which could affect the content, and all legal disclaimers that apply to the journal pertain.

CONFLICT OF INTEREST STATEMENT

The authors affirm that they have no financial affiliation or involvement with any commercial organization that has direct financial interest in any matter included in this manuscript.

and Shung, 1995, Lin, et al., 1999, Linder-Ganz and Gefen, 2004, Davis, et al., 2003, Gareis, et al., 1992, Hawkins and Bey, 1997, Muhl, 1982, Van Loocke, et al., 2006), many have used the load and displacement seen across the entire musculotendinous unit to derive stress and strain (Anderson, et al., 2001, Gosselin, et al., 1998, Lin, et al., 1999, Linder-Ganz and Gefen, 2004, Davis, et al., 2003, Gareis, et al., 1992, Hawkins and Bey, 1997, Muhl, 1982), making it difficult to isolate the properties of the muscle tissue itself. That these studies used different muscles from several different species increases the difficulty of generalization. Further, the only studies that have reported experimentally-determined transverse material properties have been under compression (Aimedieu, et al., 2003, Mathur, et al., 2001, Bosboom, et al., 2001, Van Loocke, et al., 2006). In the very few studies known to report shear properties, the study by Gao et al was limited to an examination of epimysium (Gao, et al., 2008), and the studies by Van Loocke examined muscle samples under a compression applied 45° from the fiber direction (Van Loocke, et al., 2006, Van Loocke, et al., 2008).

The aim of the current study was to collect a set of data that will allow the characterization of skeletal muscle as a three-dimensional transversely isotropic material. Stress-strain relations are derived from uniaxial tension tests of muscle under LE, TE, and LS and can be used to build computational models of muscles of varying geometries.

MATERIALS AND METHODS

Nine New Zealand White rabbits were obtained with institutional approval. Hind limbs were amputated mid-femur and stored in a freezer within one hour of sacrifice. From the 18 available fresh-frozen hind limbs, 6 limbs each were used for LE, TE, and LS tests. Tests were performed on extensor digitorum longus (EDL) muscles, chosen for its regular cross-section and low pennation angle (Lieber and Blevins, 1989). To ensure that only muscle tissue was tested, aponeuroses were carefully dissected away (Figure 1) using a blade breaker (Fine Science Tools, Foster City, CA). Unless otherwise indicated, specimen length, width, and thickness were measured before clamping using a micrometer. As the compliance of the muscle tissue was such that trimming samples for TE testing resulted in irregular cross-sections, samples for these tests were trimmed to the length of the clamps after mounting them in the test fixtures. All material tests were performed at a strain rate of $0.05\% \text{s}^{-1}$ to minimize viscoelastic effects (Van Loocke, et al., 2006). Saline was applied to the specimens to maintain tissue moisture throughout testing.

Longitudinal and Transverse Extension Tests

Material testing under the LE and TE conditions was performed on an MTS 312 material test device (MTS, Eden Prairie, MN). Specimens were mounted to the test device using sinusoidally-grooved clamps. LE specimens were gripped to provide deformation along muscle fiber direction (Fig 2a); TE specimens were gripped in the clamp jaws such that applied extension would occur perpendicular to the fiber direction (Fig. 2b). To ensure that load passed through the entire cross-section of the TE test specimens, muscle lengths were cut to the width of the clamps (25.4 mm). Force measurements were sampled at 20 Hz using a 111.2-N load cell (Lebow, Columbus, OH), and the second Piola-Kirchoff stress was calculated as the force divided by the initial cross-sectional area. Material elongation was determined using crosshead displacement. Since the muscle was deformed beyond the small strain range, Green strain was used as a deformation measure and calculated as:

$$e = \frac{1}{2}(\lambda^2 - 1)$$

where λ is the stretch ratio,

$$\lambda = \frac{l_i}{l_o}$$

where l_o is the original crosshead displacement and l_i is the current crosshead displacement. Extension samples were strained at $0.05\%\,s^{-1}$ until either failure or the stroke length limit of 50mm was reached.

Longitudinal Shear Tests

Longitudinal shear tests were performed on an ElectroForce 3200 test device (Bose Corporation, Eden Prairie, MN). Cyanoacrylate was used to glue the superficial and deep faces of the muscles to plexiglas platens which were, in turn, screwed to shear test fixture uprights. Fixture uprights were offset, ensuring that the measured force passed through the specimen midsection (Fig. 2C). Force measurements were sampled at 20 Hz using a 45-N load cell (Sensotec, Columbus, OH); the second Piola-Kirchoff stress was calculated as the applied force divided by the initial cross-sectional area. As with the elongation tests, deformation measurements were obtained using crosshead displacement and Green shear strain was used and calculated as:

$$\gamma = \tan\left(\frac{d}{t}\right)$$

where d is the longitudinal displacement of the material, and t is the thickness of the test specimen. Samples were strained at $0.05\%\,s^{-1}$ until either failure or the stroke length limit was reached.

Material Properties Definition

Linear modulus, ultimate stress, and failure strain under LE, TE, and LS were determined from their respective stress-strain plots from individual trials. Material properties for the linear region of the stress-strain curve were determined using the method described by Haut Donahue et al. (Donahue, et al., 2001). Summary statistics were calculated using a one-way ANOVA, with significance set at $p<0.05$.

RESULTS AND DISCUSSION

Typical stress-strain results for LE, TE, and LS tests are shown in Figure 3. The linear modulus of the EDL under LE is significantly higher than under either TE or LS (Table 1); no significant difference was found between the modulus for TE and LS.

As the displacement of 10 mm did not cause material failure of the EDL under LS, failure properties are reported for LE and TE only. Failure under LE or TE was observed as a separation of muscle fibers within the muscle tissue (as opposed to a complete midsubstance failure of the tissue). It is important to note that muscle fiber separation was not observed until after the maximum load in the TE specimens was reached (Figure 3). Therefore, the material microstructure was continuous up to the maximum load. The ultimate stress was significantly higher under LE; conversely, the failure strain was significantly higher for specimens under TE (Table 1). Results had a statistical power of > 0.90. Additionally, while material failure did not occur during LS testing, the technique of cementing the specimens to the platens was very efficacious. Visual inspection of the post-test samples revealed that the tissue of the cemented region remained affixed to the platens, and that the cement did not penetrate beyond the surface.

The amount of variability in biological experimental data should always be accounted for when assessing experimental data. As the coefficient of variation (Table 1) was less than 1, the data can be considered low-variance. Additionally, the linear modulus values for each test direction lie within the 10th and 90th percentile of the sample distribution (Figure 4).

Results of this study indicate a higher linear modulus in LE, than in either the TE or LS. Given the large disparity between the linear moduli found in this study, the larger modulus for LE (447 kPa) compares favorably with the 100–700 kPa range Mathur (Mathur, et al., 2001) described during low-magnitude indentations of murine skeletal muscle cells. Likewise, the order of magnitude reduction seen in the transverse modulus of 22 kPa from the current study correlates with the reported value of 75 kPa reported by Linder-Ganz and Gefen (Linder-Ganz and Gefen, 2004).

The effect of aponeurosis on the linear modulus under LE and TE can be seen through comparison with work performed previously (Morrow, et al., 2008). In the previous study uniaxial tensile elongation tests were performed on medial gastrocnemius muscles from New Zealand White rabbits using the same protocol as this study. The resulting linear moduli from LE and TE tests (767 kPa and 81 kPa, respectively) are significantly higher than the moduli reported in the current study ($p<0.01$ and $p<0.02$, respectively). This is not an unexpected result, with the mechanical response of the muscle reinforced by the collagenous aponeurosis. Additionally, since the longitudinal and transverse moduli properties of tendon have been reported as being 2700 kPa and 50 kPa, respectively (Blemker and Delp, 2005), it was not surprising that the contribution of the aponeurosis was comparatively larger in the longitudinal direction. These results suggest that the presence of aponeurosis would strongly influence how the tissue may be represented and may nullify the assumption of transverse isotropic material symmetry. However, because the aponeuroses were dissected from test samples, transverse isotropy can still be assumed in the tissue corresponding to the muscle fiber axis.

Results of the current study indicate that the ultimate stress in muscle under LE is significantly higher than under TE; the converse is true for the failure strain. Van Ee (Van Ee, et al., 2000) performed a study in which rabbit tibialis anterior muscles were loaded to failure in the longitudinal direction, reporting an ultimate stress of 460 kPa and a failure strain of 0.31. The larger ultimate stress and the lower failure strain may, at least in part, be attributable to the presence of aponeurosis in Van Ee test specimens. The additional strength provided by the tendinous aponeurosis, giving the higher ultimate stress, also constrains the deformation of the softer muscle material at failure.

Comparisons with studies of skeletal muscle under compression (Van Loocke, et al., 2006, Van Loocke, et al., 2008) suggest that skeletal muscle tissue is a bimodular material. Contrary to the findings of the current study, under the same strain rate, Van Loocke et al. found the cross-fiber modulus to be higher than the fiber-direction modulus. Additionally, the moduli found were substantively lower than those of the current study; the longitudinal and transverse modulus of fresh porcine muscle, calculated for a strain of 0.3, were found to be 2.04 and 4.56 kPa, respectively.

One limitation of this study is that testing was performed on fresh-frozen samples. Previous studies have examined the effects of freezing and/or rigor on skeletal muscle tissue material (Van Ee, et al., 2000) (Van Loocke, et al., 2006). However, a comparison of the linear modulus of specimens tested under longitudinal extension one-hour postmortem with specimens tested one hour after thawing from a pre-rigor freeze (Van Ee et al., 2000) revealed no apparent difference; this suggests that the results of the current study offer a good estimation of skeletal muscle material properties. However, further testing may need to be performed on samples within 4 hours of sacrifice before material properties can be considered suitable for modeling

in vivo musculature. Additionally, the quasi-static rate of extension used in this study is likely well below rates seen under physiological conditions. This data may be augmented by subsequent studies performed at strain rates typical experienced in vivo. Lastly, at a testing length:width ratio of approximately 1:5, the aspect ratio of the TE specimens was less than optimal ratio of 5:1 preferred to ensure that all clamping effects are eliminated in elongation tests in accordance with St. Venant's principle (Timoshenko and Goodier, 1951). Testing was performed on specimens with this geometry due to difficulties that would be encountered in cutting out specimen geometries to the small dimensions that would be required to achieve this aspect ratio in a rabbit skeletal muscle.

CONCLUSIONS

This study marks the first time a set of 3D passive tensile material properties have been collected. These results show that even with the aponeurosis dissected away, skeletal muscle still has a significantly higher elastic modulus in the fiber direction than in the cross-fiber direction. The order of magnitude decrease between the elastic modulus of skeletal muscle under LE and TE is likewise demonstrated by an additional order of magnitude decrease in the elastic modulus of LS. Further, the data provided by this study are sufficient to characterize continuum models that represent skeletal muscle as transversely isotropic and hyperelastic.

Acknowledgments

REFERENCES

Aimedieu P, Mitton D, Faure JP, Denninger L, Lavaste F. Dynamic stiffness and damping of porcine muscle specimens. Medical Engineering & Physics 2003;25(9):795–799. [PubMed: 14519353]

Anderson J, Joumaa V, Stevens L, Neagoe C, Li Z, Mounier Y, Linke WA, Goubel F. Passive stiffness changes in soleus muscles from desmin knockout mice are not due to titin modifications. Pflugers Archiv-European Journal of Physiology 2002;444(6):771–776. [PubMed: 12355177]

Anderson J, Li ZL, Goubel F. Passive stiffness is increased in soleus muscle of desmin knockout mouse. Muscle & Nerve 2001;24(8):1090–1092. [PubMed: 11439386]

Blemker SS, Delp SL. Three-dimensional representation of complex muscle architectures and geometries. Ann Biomed Eng 2005;33(5):661–673. [PubMed: 15981866]

Boriek AM, Capetanaki Y, Hwang W, Officer T, Badshah M, Rodarte J, Tidball JG. Desmin integrates the three-dimensional mechanical properties of muscles. American Journal of Physiology-Cell Physiology 2001;280(1):C46–C52. [PubMed: 11121375]

Bosboom EMH, Hesselink MKC, Oomens CWJ, Bouten CVC, Drost MR, Baaijens FPT. Passive transverse mechanical properties of skeletal muscle under in vivo compression. Journal of Biomechanics 2001;34(10):1365–1368. [PubMed: 11522318]

Davis J, Kaufman KR, Lieber RL. Correlation between active and passive isometric force and intramuscular pressure in the isolated rabbit tibialis anterior muscle. J Biomech 2003;36(4):505–512. [PubMed: 12600341]

Donahue TLH, Gregersen C, Hull ML, Howell SM. Comparison of viscoelastic, structural, and material properties of double-looped anterior cruciate ligament grafts made from bovine digital extensor and human hamstring tendons (vol 123, pg 162, 2001). Journal of Biomechanical Engineering-Transactions of the Asme 2001;123(5):523–523.

Gao Y, Kostrominova TY, Faulkner JA, Wineman AS. Age-related changes in the mechanical properties of the epimysium in skeletal muscles of rats. Journal of Biomechanics 2008;41(2):465–469. [PubMed: 18031752]

Gareis H, Solomonow M, Baratta R, Best R, D'Ambrosia R. The isometric length-force models of nine different skeletal muscles. Journal of Biomechanics 1992;25(8):903–916. [PubMed: 1639834]

Gielen AWJ, Oomens CWJ, Bovendeerd PHM, Arts T, Janssen JD. A Finite Element Approach for Skeletal Muscle using a Distributed Moment Model of Contraction. Computer Methods in Biomechanics & Biomedical Engineering 2000;3:231–144. [PubMed: 11264850]

Gosselin LE, Adams C, Cotter TA, McCormick RJ, Thomas DP. Effect of exercise training on passive stiffness in locomotor skeletal muscle: role of extracellular matrix. Journal of Applied Physiology 1998;85(3):1011–1016. [PubMed: 9729577]

Hawkins D, Bey M. Muscle and tendon force-length properties and their interactions in vivo. Journal of Biomechanics 1997;30(1):63–70. [PubMed: 8970926]

Hete B, Shung KK. A Study of the Relationship between Mechanical and Ultrasonic Properties of Dystrophic and Normal Skeletal-Muscle. Ultrasound in Medicine and Biology 1995;21(3):343–352. [PubMed: 7645126]

Hill, AV. The Heat of Shortening and the Dynamic Constants of Muscle. Proceedings of the Royal Society of London, Series B.; 1938. p. 136-195.

Jenkyn TR, Koopman B, Huijing P, Lieber RL, Kaufman KR. Finite element model of intramuscular pressure during isometric contraction of skeletal muscle. Phys Med Biol 2002;47(22):4043–4061. [PubMed: 12476981]

Johansson T, Meier P, Blickhan R. A finite-element model for the mechanical analysis of skeletal muscles. Journal of Theoretical Biology 2000;206(1):131–149. [PubMed: 10968943]

Lieber RL, Blevins FT. Skeletal muscle architecture of the rabbit hindlimb: functional implications of muscle design. Journal of Morphology 1989;199(1):93–101. [PubMed: 2921772]

Lin RM, Chang GL, Chang LT. Biomechanical properties of muscle-tendon unit under high-speed passive stretch. Clinical Biomechanics 1999;14(6):412–417. [PubMed: 10521623]

Linder-Ganz E, Gefen A. Mechanical compression-induced pressure sores in rat hindlimb: muscle stiffness, histology, and computational models. Journal of Applied Physiology 2004;96(6):2034–2049. [PubMed: 14766784]

Martins JAC, Pires EB, Salvado R, Dinis PB. A numerical model of passive and active behavior of skeletal muscles. Computer Methods in Applied Mechanics and Engineering 1998;151(3–4):419–433.

Mathur AB, Collinsworth AM, Reichert WM, Kraus WE, Truskey GA. Endothelial, cardiac muscle and skeletal muscle exhibit different viscous and elastic properties as determined by atomic force microscopy. Journal of Biomechanics 2001;34(12):1545–1553. [PubMed: 11716856]

Muhl ZF. Active length-tension relation and the effect of muscle pinnation on fiber lengthening. Journal of Morphology 1982;173(3):285–292. [PubMed: 7186549]

Odegard GM, Haut Donahue TL, Morrow DA, Kaufman KR. Constitutive Modeling of Skeletal Muscle Tissue. Journal of Biomechanical Engineering. 2008In Press

Van Ee CA, Chasse AL, Myers BS. Quantifying skeletal muscle properties in cadaveric test specimens: Effects of mechanical loading, postmortem time, and freezer storage. Journal of Biomechanical Engineering-Transactions of the Asme 2000;122(1):9–14.

Van Loocke M, Lyons CG, Simms CK. A validated model of passive muscle in compression. J Biomech 2006;39(16):2999–3009. [PubMed: 16313914]

Van Loocke M, Lyons CG, Simms CK. Viscoelastic properties of passive skeletal muscle in compression: Stress-relaxation behaviour and constitutive modelling. Journal of Biomechanics 2008;41(7):1555–1566. [PubMed: 18396290]

Yucesoy CA, Koopman BH, Huijing PA, Grootenboer HJ. Three-dimensional finite element modeling of skeletal muscle using a two-domain approach: linked fiber-matrix mesh model. J Biomech 2002;35(9):1253–1262. [PubMed: 12163314]
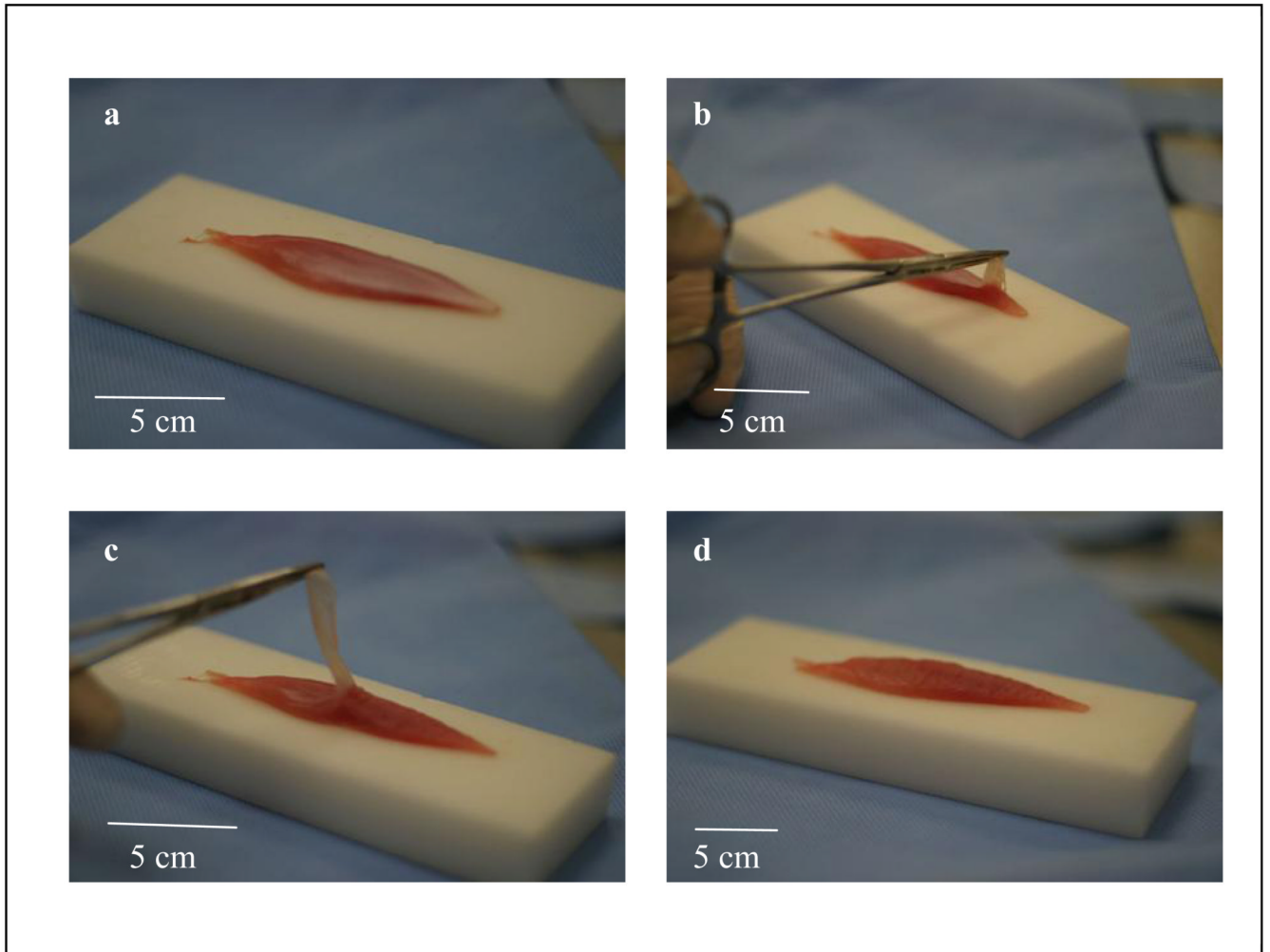
Figure 1.
Stages of aponeurosis dissection from an extensor digitorum longus: starting with (a) an intact muscle, (b) a small portion of aponeurosis is separated from the muscle near the transition to full tendon, (c) a blade breaker is used to progressively separate the aponeurosis from the muscle belly, until (d) the connective tissue is entirely separated from the muscle.
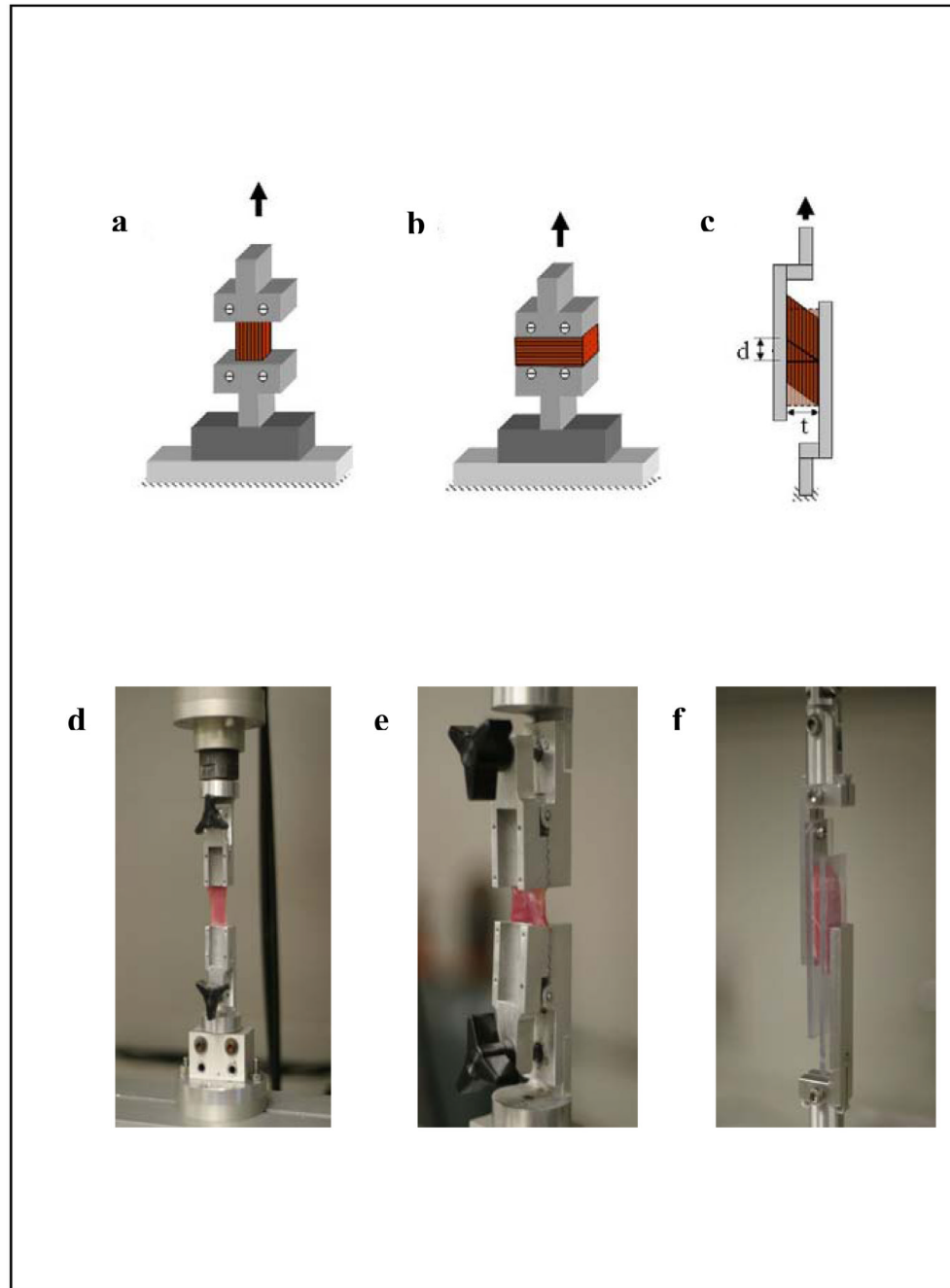
Figure 2.
Test configuration schematics for (a) longitudinal extension, (b) transverse extension, and (c) longitudinal shear tests. Photographs of (d) longitudinal extension, (e) transverse extension, and (f) longitudinal shear tests.
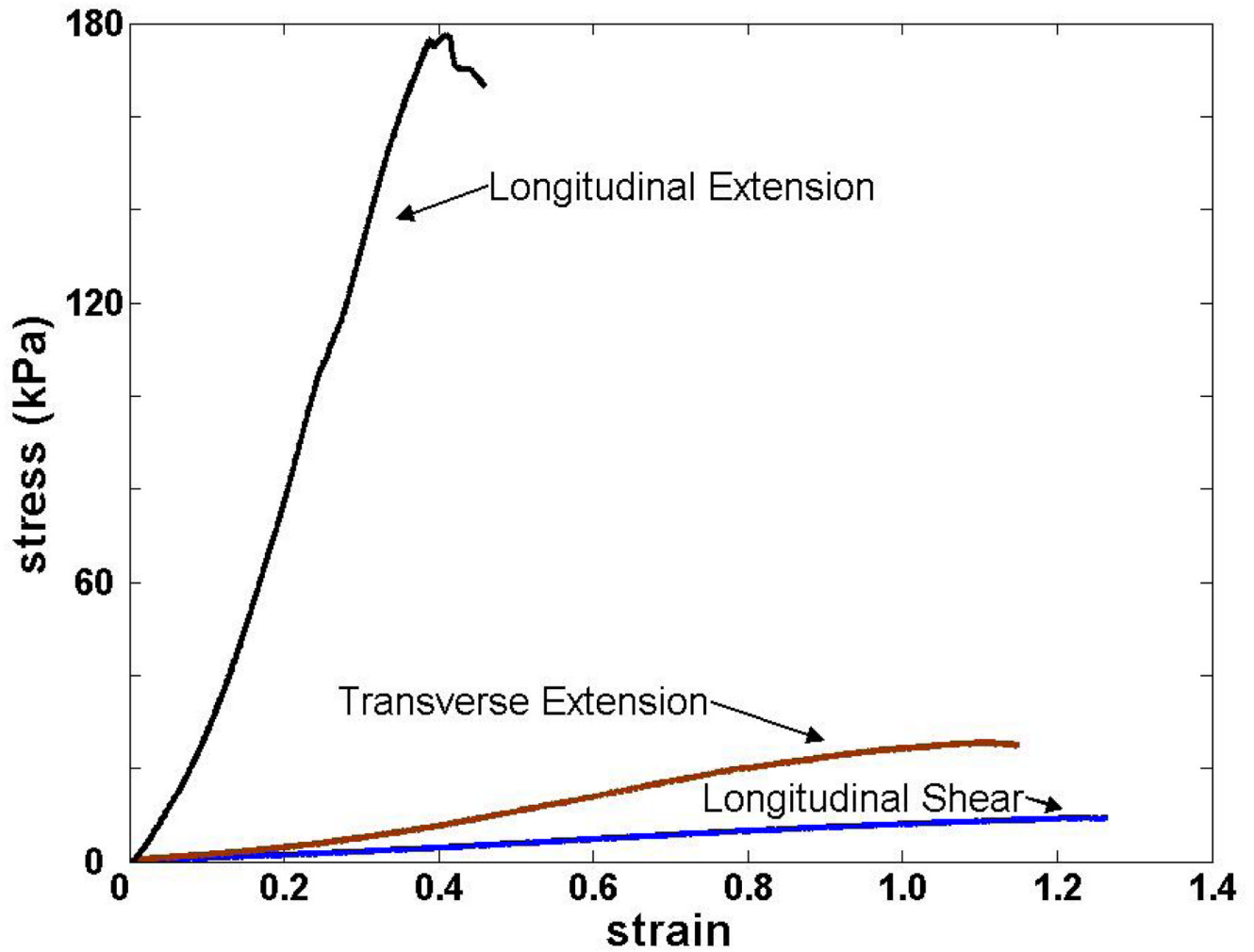
Figure 3.
Representative stress-strain curves for longitudinal extension, transverse extension, and longitudinal shear tests.
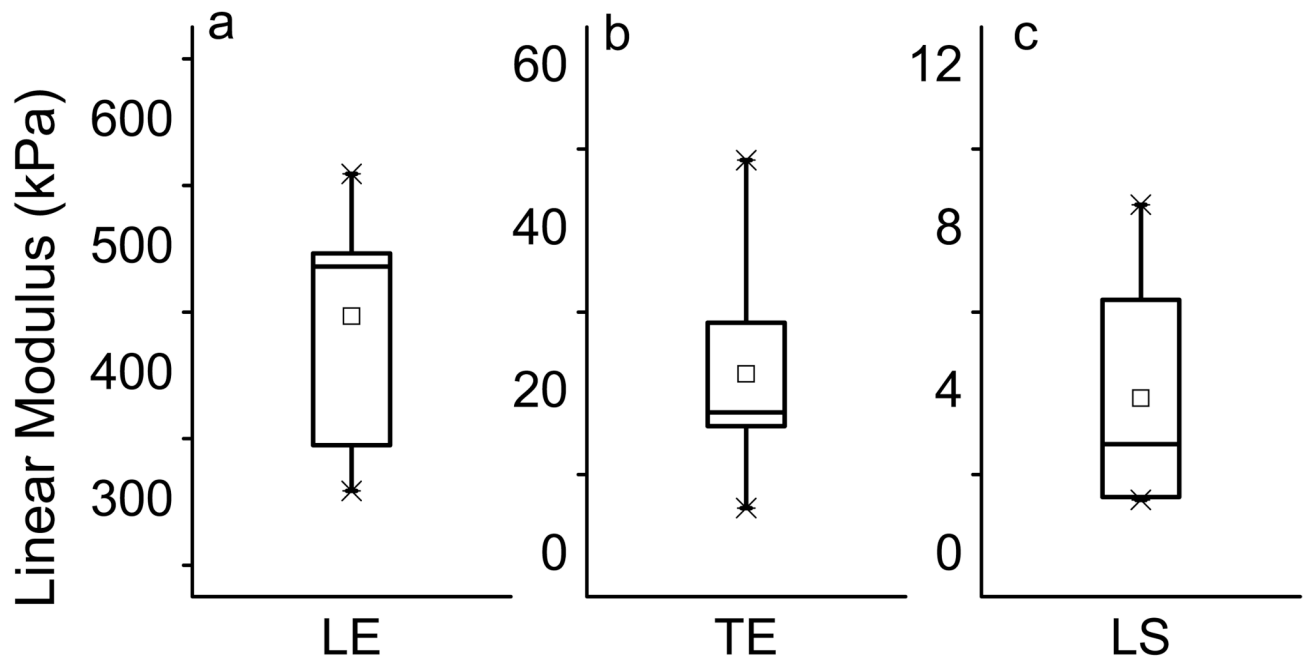
Figure 4.
Box plots of Linear Modulus for (a) longitudinal extension, (b) transverse extension, and (c) longitudinal shear tests. Minimum and maximum values are represented by Xs; whiskers connect values between the 10th and 90th percentile.

Table 1

Skeletal muscle tensile material properties

	Linear Modulus (kPa)		Ultimate Stress (kPa)		Failure Strain	
	Mean ± SD	CV	Mean ± SD	CV	Mean ± SD	CV
Longitudinal Extension	447 ± 97.7	0.218	163 ± 75.7	0.464	0.505 ± 0.222	0.440
Transverse Extension	22.4 ± 14.7*	0.656	27.5 ± 9.9*	0.360	1.82 ± 0.924*	0.508
Longitudinal Shear	3.87 ± 3.39*	0.876	NA	NA	NA	NA

Coefficient of Variability (CV) defined as standard deviation (SD) divided by the mean.

Transverse extension and longitudinal shear values for linear modulus, ultimate stress, and failure strain that differ significantly from longitudinal extension are indicated by an asterisk (*).